

# Experimental investigation of in-line tube bundles

T. Yahiaoui\*, L. Adjlout\*\*, O. Imine\*\*\*

\*Laboratoire de Mécanique appliquée, Département de Génie Maritime, Mechanical Engineering Faculty, USTO Oran, 31000 Algeria, E-mail: yahiaoui\_tayeb@yahoo.fr

\*\*Laboratoire de Mécanique appliquée, Département de Génie Maritime, Mechanical Engineering Faculty, USTO Oran, 31000 Algeria, E-mail: adjlout@yahoo.fr

\*\*\*Laboratoire de Mécanique appliquée, Département de Génie Maritime, Mechanical Engineering Faculty, USTO Oran, 31000 Algeria, E-mail: imine\_omar@yahoo.fr

## 1. Introduction

The flow within the tube bundles experiences complex unsteady behaviour. Random excitation forces can cause low-amplitude tube motion that will result in long-term-fretting-wear or fatigue. All these problems attract the attention of researchers in the whole world.

Pierson [1] and Hüge [2] systematically studied heat transfer and pressure drop both in staggered and in-line tube bundle arrangements of various configurations in cross flow of gases. Ishigai et al. [3] investigate the flow pattern for a wide range of gap ratios. It is reported that for in-line tube bundle five distinct regions are formed. However, in case of square tube bundles only three distinct flow patterns are observed. For very narrow gap ratios the free shear layer of the front of the cylinder attaches to the downstream cylinder thus stopping the Karman vortices to develop. For moderate gap ratio the Karman vortices are shed but are distorted and deflected due to downstream suppression. For very wide gap ratios regular Karman vortices are shed much like in the case of a single cylinder. Aiba et al. [4] perform experimental study on square in-line tube banks for gap ratio of 1.2 and 1.6. It is observed that the tube response of the downstream cylinders is quite different from the upstream ones.

The pressure distribution around the cylinder surface shows highly deflected flow with a stagnation point of  $45^\circ$ . The flow behaviour is asymmetric for both these configurations which are owed to the narrow gap ratios. Zukauskas and Ulinskas [5] reported extensive experimental data for heat transfer and fluid friction during viscous flow cross in-line and staggered banks of tubes under two thermal boundary conditions. Weaver and Abd-Rabbo [6] had performed visualisation study of in-line tube bundle with pitch ratio 1.5. Sayers [7] presents yet another experimental study for a four cylinder arrangement showing either a total suppression of vortex shedding or an asymmetrical pattern for very narrow gap ratios. Traub [8] conducts open wind tunnel experiments to study the influence of turbulence intensity on pressure drop in in-line and staggered tube bundles at various Reynolds numbers. It is observed that the drag coefficient remains more or less the same for a wide range of Reynolds numbers and only changes slightly for very high Reynolds numbers. Detailed visualisation investigations of the flow in tube bundle have been performed by Weaver, Fitzpatrick [9], Beale and Spalding [10] and Sweeney and Meskell [11]. Konstantinidis et al. [12] examined experimentally the effect of inlet flow pulsation in across flow over a tube array with an external frequency around twice that the flow pulsation activates

the flow field behind the first cylinder and increases the turbulence intensities for the first three cylinders. Benhamadouche and Laurence [13] performed LES calculations for the turbulent flow across the staggered tube bundle using the finite-volume method on a collocated unstructured grid. Benhamadouche S. [14] Using LES in Code Saturne for tube bundles, a database of lift and drag coefficients for various positions of a displaced tube constituted this to feed into flow induced vibrations solid/simplified-fluid software. In the case of a densely packed inline tube array (pitch/diameter = 1.5), an asymmetric mean flow solution was found, even for a nil displacement of the central tube. The asymmetric pressure signal is confirmed by experiments and a second LES on a different grid Afgan [15] had simulated numerically the problem of in-line tube bundles using RANS models and LES.

## 2. Experimental facility

The Wind Tunnel shown in Fig. 1 is of a closed circuit, horizontal return type. The Closed Circuit Wind Tunnel is of conventional design and has advantages over a similar open circuit design. These include; a higher maximum velocity, lower power consumption and lower noise level. It is driven by an A.C motor and axial flow fan that forces air around the circuit and produces a maximum velocity of 60 m/s.

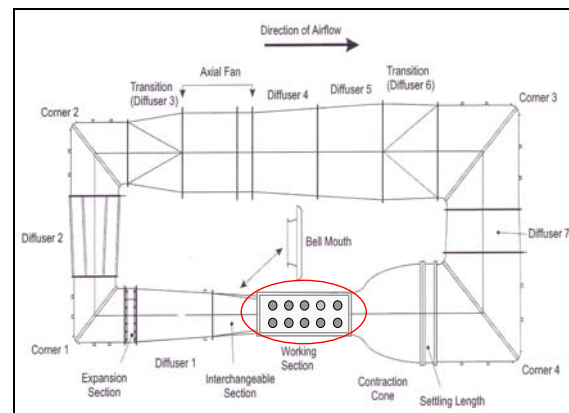


Fig. 1 Wind tunnel used fitted with the new working section

Fig. 2 shows the new working section of the tube bundle model used. The bundle consists of seven rows of PVC tubes of outer diameter of 40 mm arranged in an online array. As shown in the figure, each row has seven

full tubes. Half tubes were also mounted along the bottom and top walls of the test model alternately to simulate an infinite tube bundle and minimize the wall boundary layer.

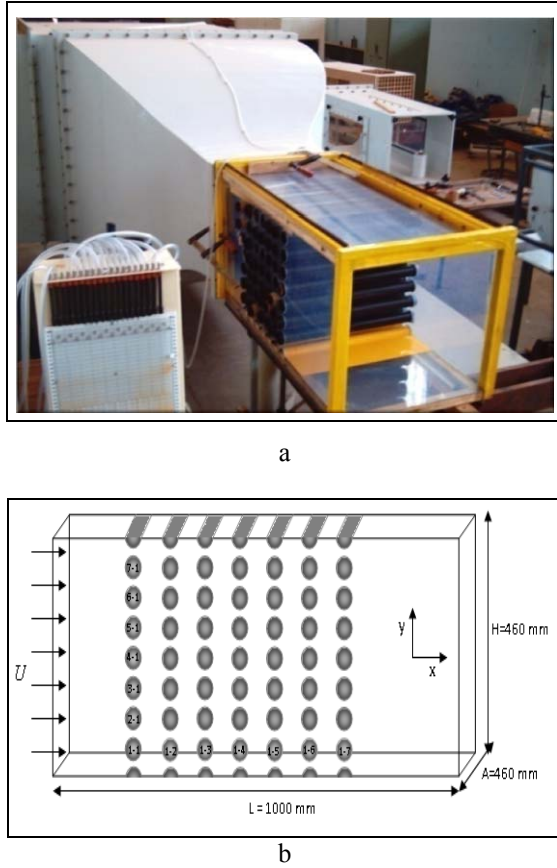


Fig. 2 New working section and the geometrical features of the tube bundle

### 3. Results and discussions

The experimental tests were performed for the following physical parameters:

- reynolds number = 35500 (based on diameter and gap bulk velocity);
- free stream and Gap bulk velocity:  $U_\infty = 3.1321$  m/s,  $U_g = 10.2505$  m/s ( $U_\infty$  Mean flow velocity,  $U_g$  Gap bulk velocity);
- sampling time = 1 second;
- pitch ratio,  $P/D = 1.44$  ( $P = T = 57.6$  mm,  $D = 40$  mm).

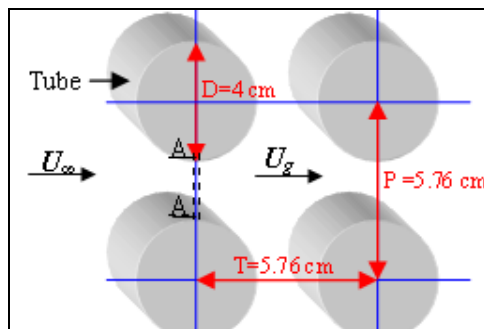


Fig. 3 Pitch ratios of tube bundles

The geometrical characteristics of the tube bundle are presented in Fig. 3

The pressure measurements were carried out for the nine tubes as shown in Fig. 2, b. The pressure tapping locations ( $p_1, p_2, \dots, p_{15}$ ) and the length of the tube (450 mm) are shown in Fig. 4, a.

The pressure measurements were performed using a TE44 DPS differential pressure scanner (Fig. 4, b). The latter pressure scanning box allowed sequential selection of up to 20 pressure tapings. The display unit links to a computer, loaded with DATASLIM software for data analysis and logging of result. The uncertainty of the pressure measurement was 0.05 mm H<sub>2</sub>O.

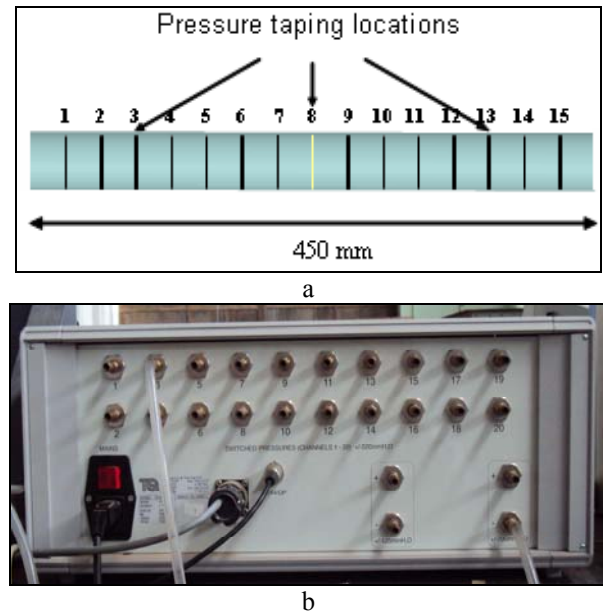


Fig. 4 Pressure tapping locations and TE44 DPS

For finite cylinders the mean pressure on the cylinder surface is also a direct result of free end interference. Park and Lee [16] reported that the mean pressure on the windward surface increases as we move to the fixed end. This is due to the fact that the vortices shed from two sides of the cylinder become dominant. On the leeward side however near the free end the mean pressure is greatly reduced.

For the cylinders with both ends fixed, it had been shown that the surface pressure distribution oscillates at the vortex shedding period and that pressure variations are consistent with periodic changes of the circulation around the cylinder body. The coefficient of pressure is defined as [13]

$$C_p = \frac{P_i - P_\infty}{0.5\rho U_g^2} \quad (1)$$

where,  $P_i$  is the surface pressure,  $P_\infty$  the static pressure and  $0.5\rho U_g^2$  the dynamic pressure.

$$\left. \begin{aligned} U_\infty T &= U_g (T - D) \\ U_g &= \frac{U_\infty T}{(T - D)} \\ U_g &= \frac{U_\infty}{\left(1 - \frac{D}{T}\right)} \end{aligned} \right\} \quad (2)$$

$$Re = \frac{U_g D}{\nu} \quad (3)$$

where  $U_g$  is the gap velocity,  $U_\infty$  is the free stream or the inlet velocity,  $T$  as defined earlier is the vertical distance between tubes centre lines and  $D$  is the tube diameter.

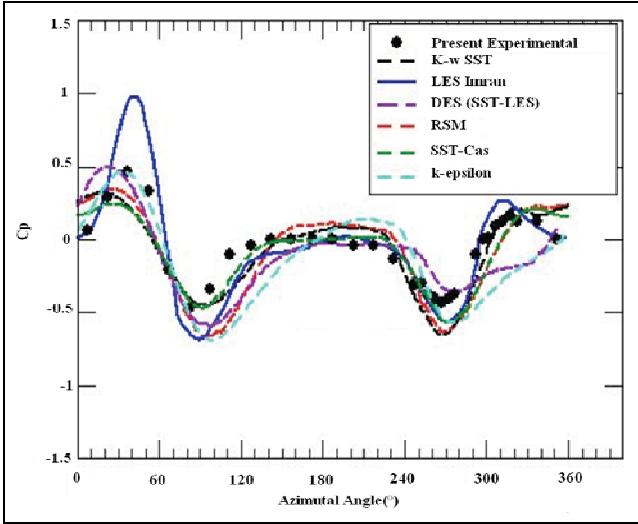


Fig. 5 Mean pressure distribution around the centre tube, comparison between the 3D URANS models and LES

Fig. 5 shows the evolution of normalized pressure coefficient around the central tube for gap ratio of 1.44 defined on Eq. (1).

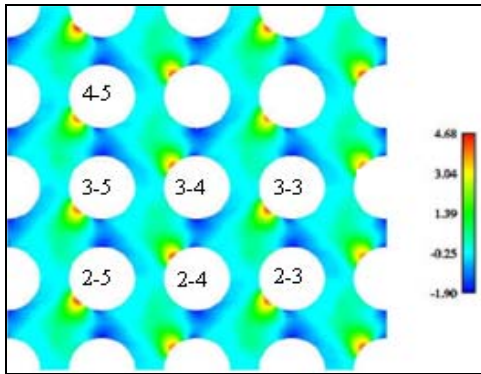
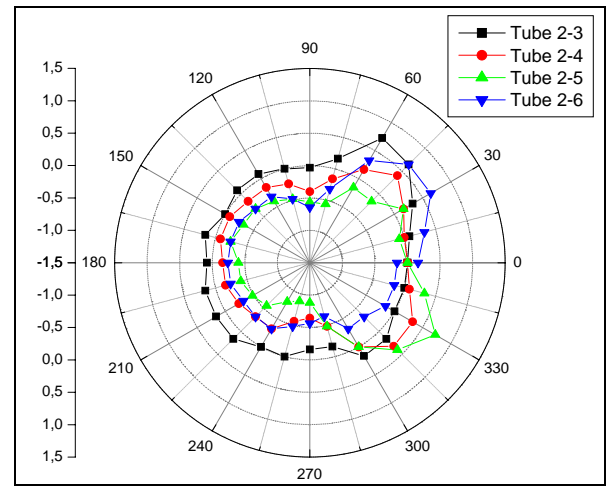


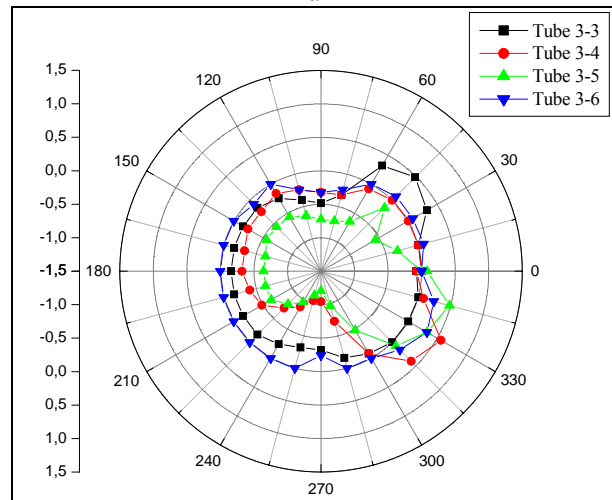
Fig. 6 Mean pressure field (the pressure drop is removed) 4 tubes cell - LES deferred n-o.c. In-line tube bundle [13]

The effect of flow deflection is observed in term of stagnation pressure region located somewhere around 45 degrees from the flow direction and in is good agreement with the present experimental results and RMS, K-wSST, DES (SST-LES), SST-Cas, K-epsilon and LES results obtained from previous study conducted by Afgan [15]. The minimum pressure is located at around 90° because of a separation of a shear layer and a recirculation region.

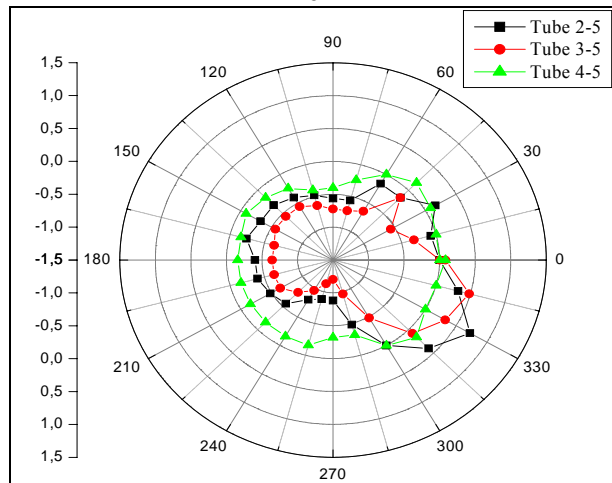
Fig. 6 exhibits the mean numerical value of the pressure for this figure. The alternating mode of the stagnation pressure is obtained again. These observations have been confirmed by the code STAR CCM which uses an explicit deferred correction algorithm in the Poisson.



a



b



c

Fig. 7 Mean pressure coefficient distribution for different tube positions: a - line 2, b - line 3 and c - cologne 5

Fig. 7 presents the mean pressure distribution around the different tube positions. The effect of flow deflection observed in the numerical study is confirmed by the experimental findings.

Fig. 8 shows the mean velocity vector field. Two recirculation bubbles coexist, a big one downstream the tube in the bottom due to the acceleration of the fluid and a small one on the top. The shear stress in the bottom of the tube is then higher than in the top.

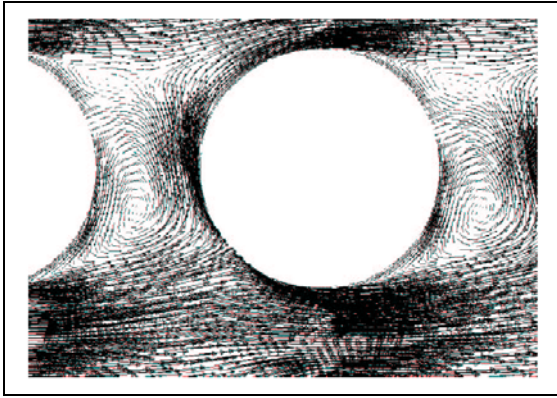


Fig. 8 The mean velocity field  $P/D = 1.44 - Re = 70\,000$  - LES implicit n-o.c. with Code Saturne. In-line tube bundle [13]

The position of the stagnation pressure region is located somewhere around  $45^\circ$ . The pressure distribution for different positions on tube is illustrated in Fig. 9 for the tubes 2.3, and 2.4. The curves show that the stagnation point location does not change and stayed around  $45^\circ$ . However, the value of the peak changes with the position of the tube. It has to be noted that for the column 3, two stagnation points exist, one situated at  $45^\circ$  and the other at  $315^\circ$ . For the tubes 2.5, and 2.6 two stagnation peaks ( $30^\circ$  and  $330^\circ$ ) are present and this is probably caused by the two contra-rotated vortices on the tube extremities as described by Aiba et al. [4]. A torsion couple is the result of the location and direction differences between the two vortices.

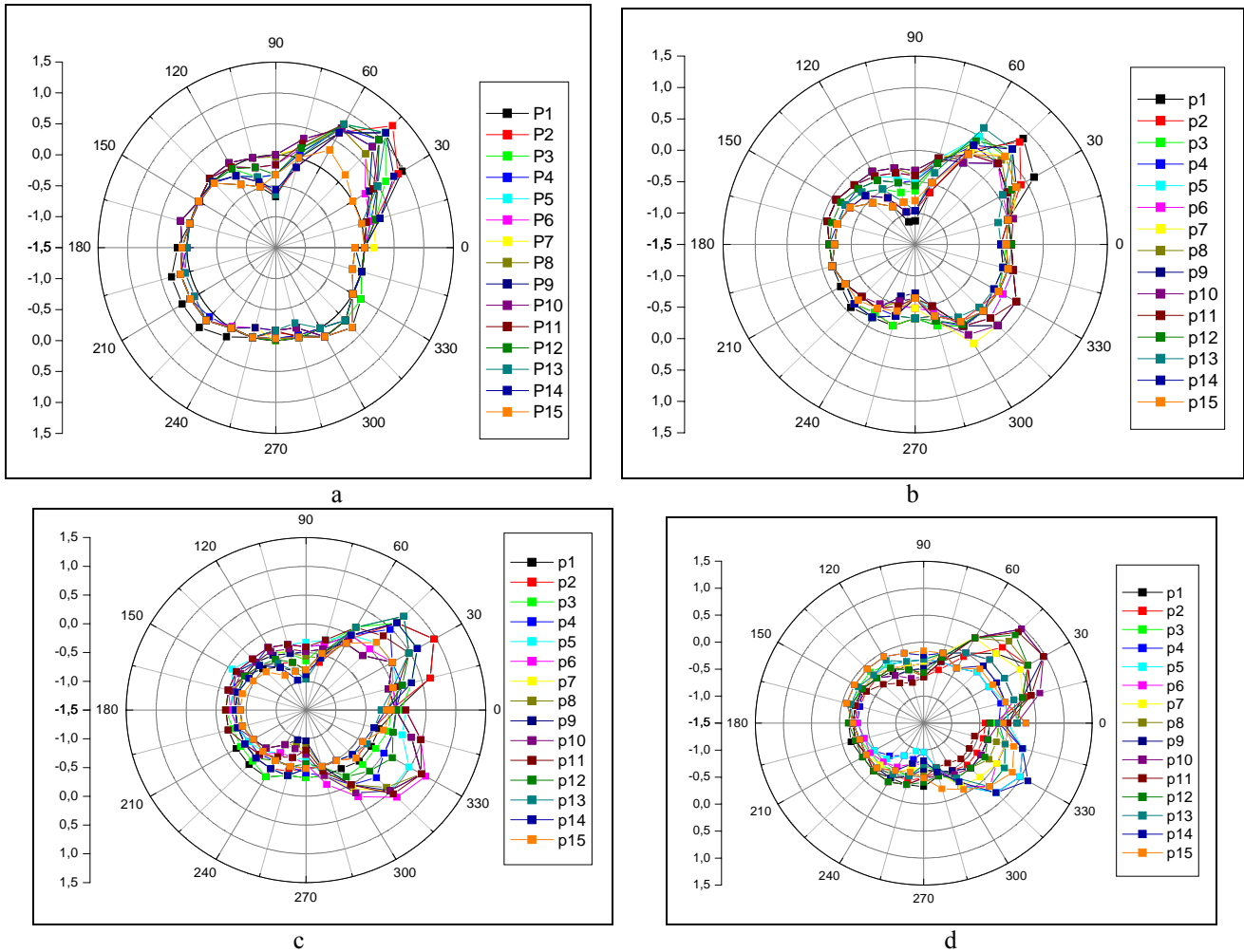


Fig. 9 Pressure coefficient distributions along the tube for different tube positions: a – tube 2-3; b - tube2-4; c- tube2-5; d - tube2-6 (Fig. 6)

Fig. 10 taken from Aiba et al. [4] shows the pressure coefficient distribution of a 7 by 7 square cylinder cluster with a gap ratio of 1.6 at Reynolds number 41000. It can be seen from figure 10 that the stagnation point is located at around 45 degrees rather than at a zero angle. It is also shown by Aiba et al. [4] that the net pressure distribution over a single cylinder inside a square cylinder array subjected to cross flow has an asymmetric distribution in both in-line and staggered cylinders.

The drag and lift forces also depend strongly on

the aspect ratio of finite cylinders. Wieselsberger [20] showed that the drag forces on the cylinder decrease as the aspect ratio of the finite cylinder becomes small. In fact most of the research in flows around cylinders revolves around lift and drag calculations since primary interest is to reduce the drag on cylinders and hence reduce the cylinder vibrations. There are two types of flow control techniques for the reduction of drag on bluff bodies; these are Active flow control techniques and Passive flow control techniques. In active techniques the flow is controlled by sup-

plying external energy such as acoustic excitation or jet blowing or some other means, but this technique over time has proved to be an expensive solution to the problem of drag reduction. The passive technique on the other hand is the one in which the flow is controlled by modifying the original shape of the geometry or by the insertion of additional control rods. This has proved to be an easier and cheaper method for the drag reduction. A recent study by Lee, et al [18] is an excellent example of this process in which a small control rod has been used to minimize the total drag force on the cylinder.

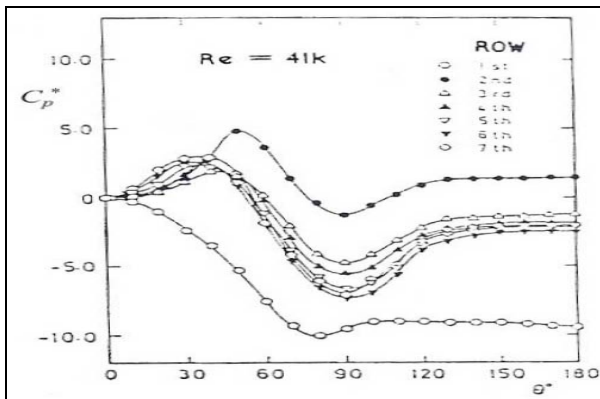


Fig. 10  $C_p$  profile for a square array 1.6 x 1.6 at  $Re = 41000$  [4]

The experimental results of Nagata [19] compare very well with that of preliminary study of Kawamura et al. [20]. For a smooth cylinder at Reynolds number 1200 Kawamura et al. [20] state that previous experiments have revealed a value for a critical Reynolds number and boundary layer thickness. This is reported to be  $Re_c = 30000$  with a boundary layer thickness of 0.5% of the radius of the cylinder at  $90^\circ$  from the stagnation point. This paper also provides good data on lift and drag (instantaneous and RMS) and pressure distributions along the cylinder surface for a wide range of Reynolds number.

The drag coefficients are presented for different pressure tapping locations on the tube in Fig. 11 for the tubes 2-3, 2-4, 2-5 and 2-6. It is clearly seen that the drag coefficient of the first tube is higher than the drag of all the other tubes. This finding is valid for all the Reynolds number investigated.

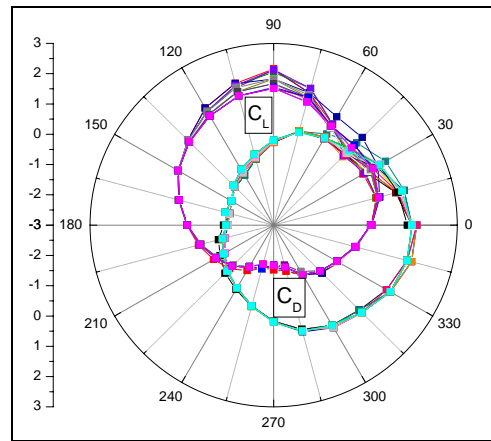
Fig. 11 gives a typical example in which form drag coefficient  $C_D$  for  $1.44 \times 1.44$ .  $C_D$  of the first cylinder is remarkably high but that of the second and downstream cylinders is nearly equal to 0.20 at the second tube (tube 2-3).

Table

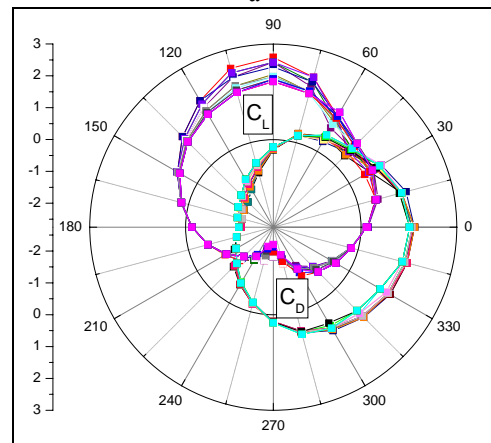
Drag coefficients for  $P/D = 1.44$  and  $Re = 35500$ . In-line tube bundle

Case	$C_D$
Exp.tube 2-3	0.200
Code_Saturne With $L_z = D$	0.339
Code_Saturne With $L_z = 2D$	0.35

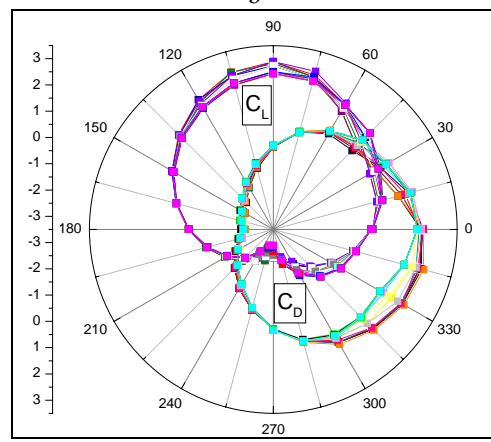
The mean value of the drag coefficient for the pressure forces is summarized in Table. The  $C_D$  is calcu-



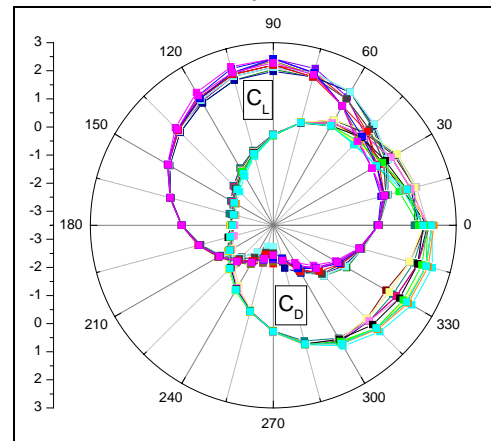
a



b



c



d

Fig. 11 Drag and lift coefficients for  $P/D = 1.44$  and  $Re = 35500$ . In-line tube bundle: a – tube 2-3; b – tube 2-4; c – tube 2-5; d – tube 2-6

lated by integral SIPSON methods, of the pressure coefficient ( $C_p$ ). This result is compared with the numerical simulation of Benhamadouche et al [13]. The results show a good agreement between the experimental and the LES simulation.

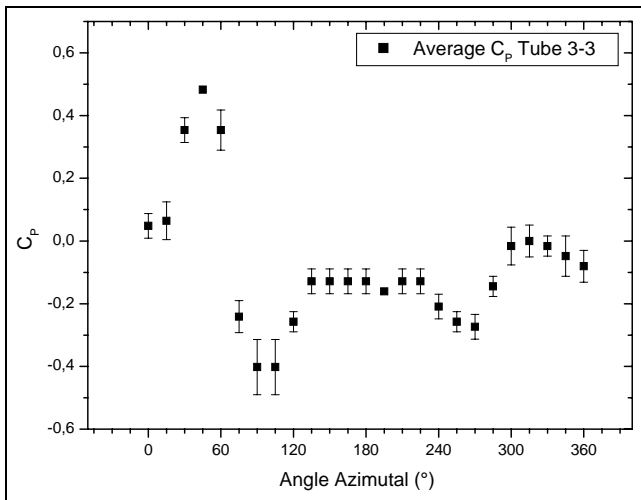


Fig. 12 Average CP tube 3-3

Fig. 12 shows the value of the root mean square RMS of the pressure coefficient values on the tube 3-3.

#### 4. Conclusions

The following conclusions have to be drawn from the present work:

##### 1. Pressure coefficient:

- The flow across in-line tube bundles is found to be asymmetric and transient.
- A satisfactory comparison of the different models used is found with the present experimental results.
- Stagnation point is located somewhere around 45 degrees. It agrees with LES of (Afgan2007 [15]).
- For the column 3, two stagnation points exist, one situated at 45° and the other at 315°.

##### 2. Drag coefficient:

- The drag coefficient for the first tube is remarkably higher than the drag for all the other tubes.
- A decrease in the drag coefficient for tube 3 and 6 for all Reynolds number is noticed.

The experimental results showed a good agreement with the prediction computing. Nevertheless, the values of drag measured for some tubes are very different from that given by the forecast calculation. This affects the calculation of losses pressure in the beam tube.

#### References

1. **Pierson, O.** Investigation of influence of tube arrangement on convection heat transfer and flow resistance in cross-flow of gases in tube banks.-ASME Trans., 1937, 59, p.563-572.
2. **Huge, E.** Experimental investigation on the effect of equipment size of heat transfer and flow resistance in cross-flow of gas over tube bank.-ASME Trans., 1937, 59, p.573-582.
3. **Ishigai, S., Nishikawa, Yagi E.** Structures of Gas flow and vibration in tube banks with tube axes normal to flow.-Inst. Symp. on Marine Engineering, Tokyo, in Flow induced vibration of circular cylinder structures by Chen, S. S. 1-5-23 to 1-5-33, 1973.
4. **Aiba, S., Tsuchida, H. Ota, T.** Heat transfer around tubes in in-line tube banks.-Bull JSME, 1982, 25, p.919-926.
5. **Zukauskas, A., Ulinskas, R.** Heat Transfer in Tube Banks in Crossflow, Hemisphere, Washington, DC, 1988.
6. **Weaver, D.S., Abd-Rabo, A.** A flow visualization study of a square array of tubes in water cross-flow.-J. Fluids Engineering, 107. 354-63; in Flow around circular cylinders Vol 2: Applications by Zdravkovich, M. M., 1985.
7. **Sayers, A.T.** Flow interference between four equispaced cylinders when subjected to a cross flow.-Journal of Wind Engineering and I. Aerodynamics, 31, 1988, p.9-28.
8. **Traub, D.** Turbulent heat transfer and pressure drop in plain tube bundles -Chem. Engineering Process, 1990, 28, p.173-181.
9. **Weaver, D.S., Fitzpatrick, J.A.** A review of cross flow induced vibrations in heat exchanger tube arrays. -Journal of Fluids and Structures, 1988, 2, p.73-93.
10. **Beale, S.B., Spalding, D.B.** A numerical study of unsteady fluid flow in In-line and staggered tube banks, -Journal of Fluids and Structures, 1999, 13, p.723-754.
11. **Sweeney, C., Meskell, C.** Numerical simulation of vortex shedding in tube arrays. -In: Proceedings of IMECE, ASME Int. Mech. Eng., Congress and Exposition. -New Orleans, Louisiana, 2002.
12. **Konstantinidis, E., Castgla, D., Balabanis, S., Yianeskis, M.** On the flow and vortex shedding characteristics of an inline tube bundle in steady and pulsating crossflow.-Transactions of IChemE, Part A, Chemical Engineering Research and Design, 2000, 78(8), p.1129-1138.
13. **Benhamadouche, S. Laurence, D., Jarrin, N., Afgan, I., Moulinec, C.** Large Eddy Simulation of flow across in-line tube bundles.-NURETH-11 (Nuclear Reactor Thermal-Hyd.), 405, Avignon FR, 2005.
14. **Benhamadouche, S.** LES coarse LES and transient RANS comparisons on the flow across a tube bundle. -International Journal of Heat and Fluid Flow, 2003, 24, p.470-479.
15. **Afgan, I.** Industrial Applications of Large Eddy Simulation. -Ph.D. thesis.-University of Manchester, 2007.
16. **Park, C.W., Lee, S.J.** Free end effect on the wake flow structure behind a finite circular cylinder.-Journal of Wind Engg. and I. Aerodynamics, 2000, 88. p.231-246.
17. **Wieselsberger, C.** Versuche uber den luftwiderstand gerundeter und kantiger korper (L. Prandtl, Ergebnisse Aerodyne). Versuchsanstalt Gottingen, Vol. II Liferung. P23.
18. **Lee, S.J., Lee, S.I., Park, C.W.** Reducing the drag on a circular cylinder by upstream installation of a small control rod. Fluid Dynamics Research, 2004, 34, p.233-250.
19. **Nagata, H.** Experimental study of unsteady flow past a circular cylinder started impulsively.-Ph.D. thesis. University of Nagoya, 1979.
20. **Kawamura, T., Takami, H., Kuwahara, K.** Computation of high Reynolds number flow around a circular

cylinder with surface roughness. -Bull. JSME 1986, 27(232), p.2142-2151.

T. Yahiaoui, L. Adjlout, O. Imine

## KORIDORINIO VAMZDŽIŲ PLUOŠTO EKSPERIMENTINIS TYRIMAS

### Reziumė

Šiame straipsnyje aprašomas eksperimentinis koridorinio vamzdžių pluošto tyrimas naudojant ikigarsinį oro srauto tunelį, kurio fiziniai parametrai tokie:

- Reynoldso skaičius lygus 3550 (priklausomai nuo skersmens ir vidutinio greičio siauriausioje vietoje);
- laisvo tekėjimo ir vidutinis greitis siauriausioje vietoje:  $U_{\infty} = 3.1321$  m/s,  $U_g = 10.2505$  m/s;
- eksperimento laikas – 1 s;
- žingsnio koeficientas,  $P/D = 1.44$  ( $P = T = 57.6$  mm,  $D = 40$  mm).

Slėgio pasiskirstymas išilgai 7 vamzdžių (15 slėgio matavimo taškų) buvo nustatytas keičiant azimuto kampą nuo 0 iki 360°.

Nustatyta, kad stabdymo ir kėlimo jėgos yra dvi žadinimo jėgos komponentės esant skersiniam tekėjimui.

Šie rezultatai gerai sutapo su skaitinio tyrimo rezultatais, gautais tiriant vamzdžių pluoštą, kurio centrinio vamzdžio žingsnio koeficientas yra 1.5. Tekėjimo nukrypimo efektas buvo pastebėtas slėgio stagnacijos zonoje apie 45° nuo srauto krypties. Šio stagnacijos taško nukrypimą buvo taip pat yra pastebėję Afgano ir Benhamadouche.

T. Yahiaoui, L. Adjlout, O. Imine

## EXPERIMENTAL INVESTIGATION OF IN-LINE TUBE BUNDLES

### Summary

In the present paper, an experimental investigation of in-line tube bundles is carried out using a subsonic wind tunnel for the following physical parameters:

- Reynolds number = 35500 (based on diameter and gap bulk velocity);
- free stream and Gap bulk velocity:  $U_{\infty} = 3.1321$  m/s,  $U_g = 10.2505$  m/s;
- sampling time = 1 second;
- pitch ratio,  $P/D = 1.44$  ( $P = T = 57.6$  mm,  $D = 40$  mm).

The pressure distributions along the seven tubes (15 pressure tapings) were determined for a variation of the azimuthal angle from 0 to 360°.

The drag and lift forces are the two excitations forces components in a cross flow.

A comparison of the present results with some numerical simulations performed on a tube bundle with an aspect ratio of 1.5 for the central tube has given a fairly good agreement. The effect of flow deflection is observed in term of stagnation pressure region located somewhere around 45° from the flow direction. This shift of stagnation point location is also validated from LES of Afgan and Benhamadouche.

Т. Иахиауи, Л. Адюлоут, О. Имине

## ЭКСПЕРИМЕНТАЛЬНОЕ ИССЛЕДОВАНИЕ КОРИДОРНОЙ СВЯЗКИ ТРУБ

### Резюме

В данной статье экспериментальное исследование коридорной связки труб проведено при использовании дозвукового потока воздуха со следующими физическими параметрами:

- число Рейнольдса – 3550 (в зависимости от диаметра и средней скорости в зазорах);
- скорость свободного течения и средняя скорость в зазорах:  $U_{\infty} = 3.1321$  м/с,  $U_g = 10.2505$  м/с;
- время эксперимента – 1 с;
- коэффициент шага  $P/D = 1.44$  ( $P = T = 57.6$  мм,  $D = 40$  мм).

Распределение давления вдоль 7 труб (15 точек измерения спусков давления) было определено изменяя угол азимута от 0 до 360°.

Определено, что силы торможения и подъема является компонентами возбуждающей силы при поперечном течении.

Сопоставление полученных аналитических результатов с результатами численного решения проведенных для связки труб с центральной трубой, имеющей 1.5 коэффициент шага показало хорошее соответствие. Эффект отклонения течения наблюдался в зоне стагнации давления 45° от направления потока. Это отклонение точки стагнации также отмечено Афганом и Бенхамadouche.

Received May 27, 2010

Accepted October 05, 2010

DOI: 10.5755/j02.mech.15960